J Electroceram (2006) 16:453–457
DOI 10.1007/s10832-006-9896-y

Ferroelectric behaviors of sandwich structured $PbZr_{0.52}Ti_{0.48}O_3/Pb(Mg_{1/3}Ta_{2/3})_{0.7}Ti_{0.3}O_3/PbZr_{0.52}Ti_{0.48}O_3$ thin film

Fang Li · Gregory K.L. Goh · John Wang

Abstract Sandwich structured $PbZr_{0.52}Ti_{0.48}O_3/Pb(Mg_{1/3}Ta_{2/3})_{0.7}Ti_{0.3}O_3/PbZr_{0.52}Ti_{0.48}O_3$ (PZT/PMTT/PZT) thin films have been successfully synthesized via a combined route involving sol-gel and RF magnetron sputtering. Insertion of the PMTT interlayer effectively suppressed formation of the heterogeneous "rosette" structure of PZT thin film when deposited onto $Pt/Ti/SiO_2/Si$ substrate. While both remanent polarization and coercive field were lowered for the sandwich structured films, the coercive field was reduced more significantly. Such sandwich structured films exhibit improved fatigue behavior and the relative permittivity can not be simply described as a series connection of individual components of perovskite layers.

Keywords Sandwich structure · Perovskite · Thin film

1 Introduction

Multilayered thin films consisting of successive ferroelectric layers of different compositions and structures have attracted considerable amount of attention in recent years, owing to their much improved electrical properties [1–3]. Indeed, the heterostructures can give rise to several unique phenomena that cannot be realized by the conventional single layer thin films [4–6]. Several such heterolayered systems have been investigated, for example, $PbTiO_3/Ba_{0.85}Sr_{0.15}TiO_3/PbTiO_3$ [7], $(Bi, La)_4Ti_3O_{12}/Pb(Zr, Ti)O_3/(Bi, La)_4Ti_3O_{12}$ [8], $PbTiO_3/PbZr_{0.53}Ti_{0.47}O_3/PbTiO_3$ [9]. Although the ferroelectric and dielectric behaviors of these heterolayered thin films were reported, they have not yet been properly studied for various film texture parameters and physical origins behind the observed electrical properties. It will therefore be of considerable interest to properly understand both the structural parameters and operating mechanisms in the heterolayered thin films.

$PbZr_{0.52}Ti_{0.48}O_3$ (PZT) thin films are well studied in conventional single layer form, because of their ferroelectric and piezoelectric properties, which promise several technologically valuable applications such as in microelectromechanical systems (MEMS), sensors, actuators and memory devices. However, they suffer from severe polarization fatigues, which significantly constrain their application ranges. In contrast, $Pb(Mg_{1/3}Ta_{2/3})_{0.7}Ti_{0.3}O_3$ (PMTT) thin films, which are close to the morphotropic phase boundary (MPB) in the binary PMT-PT system, exhibit excellent ferroelectric and dielectric behaviors, including a low coercive field, high relative permittivity and in particular much improved fatigue resistance than conventional PZT thin films [10]. It is therefore of considerable interest to investigate the feasibility of improving the ferroelectric behaviors of PZT by forming a sandwich-like structure with a PMTT nanolayer, whereby the PZT and PMTT nanolayers will interact under an E-field. In this paper, we describe a multilayered thin film structure consisting of a PMTT layer sandwiched between two PZT layers, whereby its unique polarization and dielectric behaviors are presented and discussed.

2 Experimental procedure

The PZT layer was first deposited on $Pt/Ti/SiO_2/Si$ substrate by spin coating from a precursor solution, which

F. Li · J. Wang (✉)
Department of Materials Science & Engineering,
National University of Singapore, Singapore 117576
e-mail: msewangj@nus.edu.sg

G. K.L. Goh
Institute of Materials Research and Engineering, 3 Research Link,
Singapore 117602

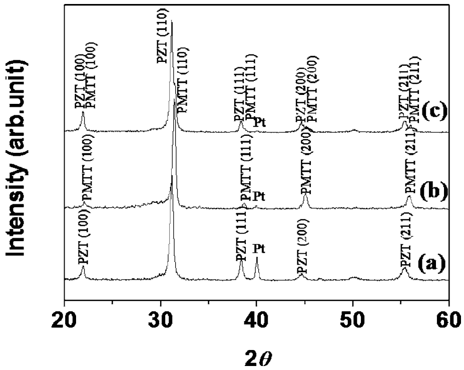

Fig. 1 XRD patterns of the sandwich structured PZT/PMTT/PZT films: (a) bottom PZT layer; (b) PMTT interlayer; and (c) top PZT layer

consisted of lead acetate trihydrate [$Pb(C_2H_3O_2)_2{\cdot}3H_2O$], titanium ethoxide [$Ti(OCH_2CH_3)_4$] and zirconium propoxide [$Zr(OCH_2CH_2CH_3)_4$] with mixed 2-methoxyethanol [$CH_3OC_2H_4OH$] and acetic acid [CH_3COOH] as the solvent. The spin-coated PZT film was dried at 300°C for 5 min, followed by thermal annealing at 500°C for 20 minutes. This process was repeated until a desirable thickness was achieved for PZT layer before thermal annealing at 650°C. $Pb(Mg_{1/3}Ta_{2/3})_{0.7}Ti_{0.3}O_3$ (PMTT) film layer was then deposited on the bottom PZT layer by RF magnetron sputtering, where PMTT target was synthesized from constituent oxides of Pb, Mg, Ta and Ti via the Columbite route [11]. During sputtering, chamber pressure was pumped below 1.0×10^{-5} Torr. Ar was then introduced to provide positive ions for sputtering. The working pressure was controlled at 25 mTorr and the RF power was maintained at 50 W. The as-deposited thin film was thermally annealed at 600°C in order to form the PMTT perovskite structure. Finally, deposition of the top PZT layer was made by following the same procedure as that for the bottom PZT layer.

Upon completion of depositing one component layer in the sandwich structure and subsequent thermal annealing, the thin film sample was characterized for phase development using X-Ray Diffractometer (XRD, CuK, Bruker, Germany) before deposition of the next component layer. Film morphology and texture were investigated using Atomic Force Microscopy (AFM, Di digital instruments, Santa Barbara, CA, USA). Prior to electrical measurement, gold top electrodes of 0.5 mm in diameter were deposited on the film surfaces through a shadow mask by sputtering. Their polarization and dielectric properties were analyzed using a Radiant Precise Workstation (Radiant Technologies, Medina, NY, USA) and an Impedance Analyzer (Solatron 1261, Farnborough, UK), respectively. Surface analysis of the sandwich structured PZT/PMTT/PZT thin film was further made by using X-ray Photoelectron Spectroscopy (XPS), assisted by the Secondary Ion Mass Spectroscopy (SIMS).

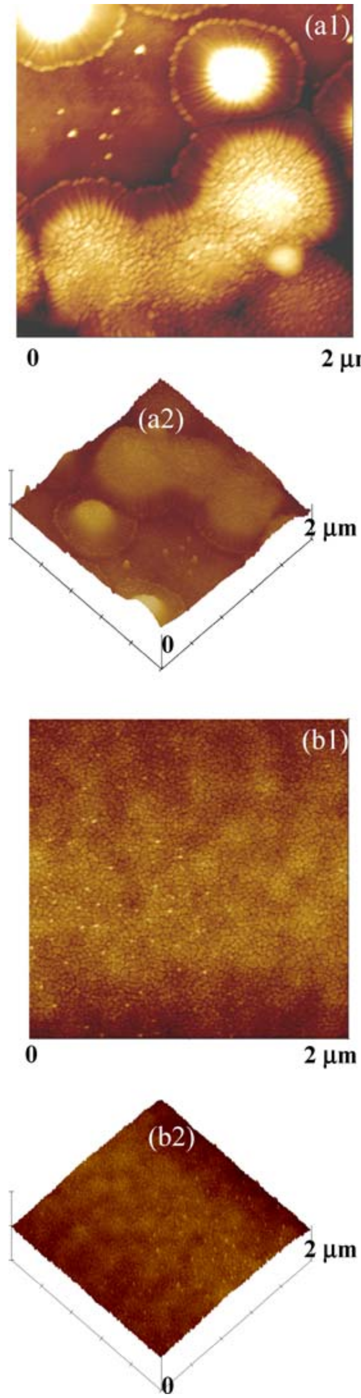

Fig. 2 Plane-view and top-view AFM images of: (a) the single layer PZT film; and (b) sandwich structured PZT/PMTT/PZT thin film of the same thickness of 380 nm

3 Results and discussion

Figure 1 shows the XRD traces of the bottom PZT layer, PMTT interlayer and top PZT layer in the sandwich structured PZT/PMTT/PZT thin film, confirming that the PZT and PMTT of perovskite structure were preserved. Indeed, the diffraction peaks at 2θ angles of 21.9°, 31.1°, 38.3°, 44.6°

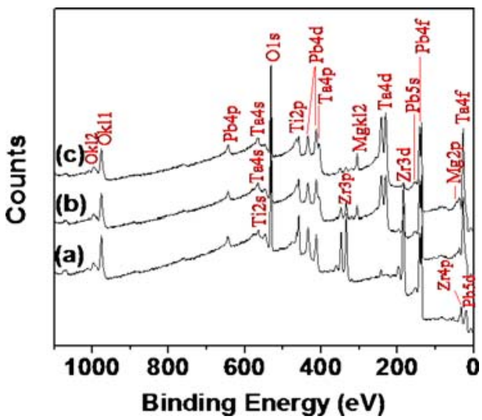

Fig. 3 XPS survey spectra for the sandwich structured PZT/PMTT/PZT thin film: (a) PZT layer; (b) interface between PZT and PMTT layers; and (c) PMTT interlayer

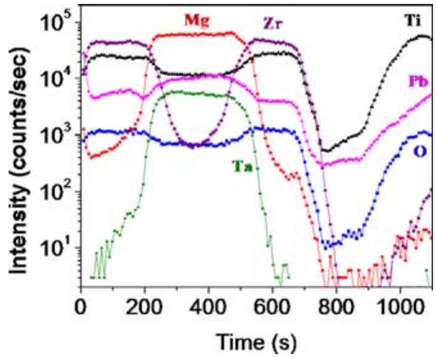

Fig. 4 SIMS depth profile of the sandwich structured PZT/PMTT/PZT thin film

and 55.3°, correspond to PZT (*100*), (*110*), (*111*), (*200*) and (*211*) planes, respectively and those peaks at 2θ angles of 22.1°, 31.5°, 38.8°, 44.9° and 56.1°, correspond to the PMTT (*100*), (*110*), (*111*), (*200*) and (*211*) planes, respectively. The two sets of diffraction peaks for PZT and PMTT are quite close to each other, due to their similarity in perovskite structure and closeness in lattice parameters (PZT: 4.07 Å and PMTT: 4.02 Å). No other secondary phases were detected in the multilayered PZT/PMTT/PZT thin film.

Figure 2 are AFM images showing the surface texture of thin film of single layer PZT (Fig. 2(a)) and that of PZT/PMTT/PZT film (Fig. 2(b)) with approximately the same thickness of 380 nm. As shown in Fig. 2(a), a "rosette"-like surface morphology was observed for the single PZT thin film derived from sol-gel route on Pt/Ti/SiO_2/Si substrate. In the sandwich structure, in contrast, as shown in Fig. 2(b), the "rosette" structure was suppressed. Both mean grain size and average roughness were reduced upon the insertion of PMTT layer. The mean grain size is 115 and 90 nm and average roughness is 8.1 and 3.2 nm for the single layer PZT and PZT/PMTT/PZT thin films, respectively. Indeed, it has been reported that the "rosette" texture is related to lead deficiency, which is induced by lead diffusion into the bottom electrode at the annealing temperature [12, 13]. The improvement in surface texture of the sandwich structured thin film is attributed to the compensation for lead deficiency in the top PZT layer by the insertion of the PMTT interlayer, whereby the "rosette" structure is suppressed in the top PZT surface of the sandwich structured PZT/PMTT/PZT thin film.

Undoubtedly, the compositions and structures of the component layers and their interactions affect the electrical behaviors of the sandwich structured thin film. XPS surface analysis was thus conducted, assisted by SIMS depth profile measurement. The survey scans of XPS spectra along three different depths confirmed the preservation of the three component layers, as shown in Fig. 3. By curve fitting from

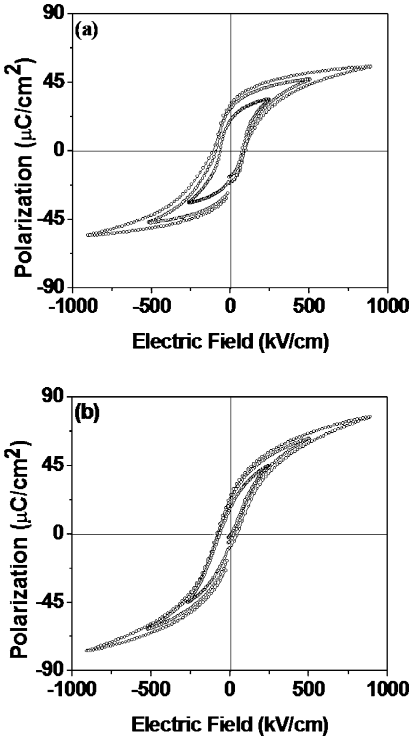

Fig. 5 P-E hysteresis loops of (a) the single layer PZT; and (b) sandwich structured PZT/PMTT/PZT thin film with the same thickness of 380 nm

the high-resolution XPS spectra, the peaks of $Pb4f_{7/2} = 137$ eV, $Zr3d_{5/2} = 183$ eV, $Ti2p_{3/2} = 458$ eV, $Mg2p = 51$ eV and $Ta4f_{7/2} = 27$ eV are close to the reported values [14–16]. As shown by the SIMS depth profile in Fig. 4, there is a degree of inter-diffusion between the bottom PZT layer and the Pt electrode. A broader mixed region between the bottom PZT layer and PMTT interlayer was also observed, which is attributed to the surface roughness of the bottom PZT layer. It was deposited directly onto the Pt electrode, whereby a heterogeneous "rosette" structure was expected. Further quantitative XPS analysis confirmed that the atomic ratio of Pb/(Zr + Ti) was close to 1 in the top PZT layer, and it approached to 0.95 in the bottom PZT layer.

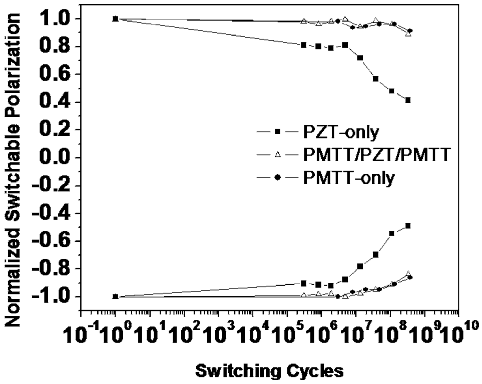

Fig. 6 Fatigue behaviors of the single layer PZT thin film, sandwich structured PZT/PMTT/PZT thin film and single layer PMTT thin film of the same thickness of 380 nm

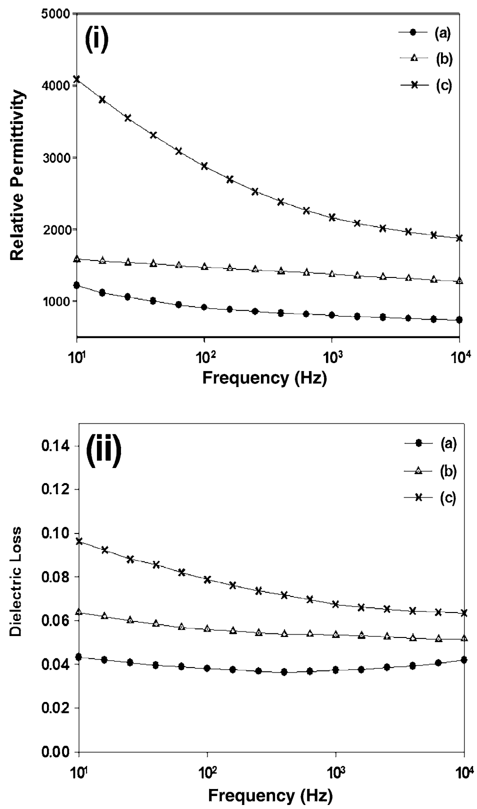

Fig. 7 Frequency dependence of (i) relative permittivity; and (ii) dielectric loss of (a) the single layer PZT; (b) sandwich structured PZT/PMTT/PZT; and (c) single layer PMTT thin films with the same thickness of 380 nm

The polarization behaviors of the single layer PZT thin film and the sandwich structured PZT/PMTT/PZT film are shown in Fig. 5. In comparison to the single layer PZT thin film, the sandwich structured PZT/PMTT/PZT film shows an apparent decrease in remanent polarization P_r and a significant fall in coercive field E_c. On one hand, this can be in part attributed to the fact that PMTT exhibits a lower P_r and E_c, as compared to PZT. On the other hand, as discussed below, the sandwich structured thin film can not be described by a simple series connection of individual components of ferroelectric layers. There can be a degree of coupling and interactions between two neighboring ferroelectric layers [17].

Fatigue behaviors of the single layer PZT, sandwich structured PZT/PMTT/PZT, and single layer PMTT thin films of the same thickness of 380 nm, were studied at 100 kHz, with a bipolar square wave amplitude of ±10 V. Figure 6 plots the degradation behaviors of normalized switchable polarization as a function of switching cycles. The single layer PZT thin film shows an apparent decay after 10^7 switching cycles and ∼60% switchable polarization is lost after 3×10^8 cycles. In contrast, the sandwich structured PZT/PMTT/PZT thin film shows much less degradation (∼15%) after 3×10^8 numbers of cycles, which is comparable to that of single layer PMTT thin film of the same thickness.

It is commonly accepted that the key parameters controlling the fatigue behavior of a ferroelectric thin film are the type and characteristics of defects occurring in the film. In particular, the loss of switchable polarization of PZT film deposited on Pt electrodes is originated from the trapping of oxygen vacancies with polarization discontinuities [18, 19]. For the sandwich structured PZT/PMTT/PZT thin film, one can consider the followings: (i) PMTT interlayer itself exhibits an improved fatigue resistance, as compared to PZT; (ii) Suppression of the "rosette" surface texture in the top PZT layer, whereby the surface roughness is reduced; and (iii) Slow-down of the inter-diffusion between the top PZT layer and the Pt electrode by the PMTT interlayer, as has been confirmed by the XPS and SIMS analyses, whereby the average defect concentration in the sandwich structured thin film is reduced.

Dielectric behaviors of the single layer PZT, sandwich structured PZT/PMTT/PZT, and single layer PMTT thin films of the same thickness of 380 nm, are shown in Fig. 7. They all show a decrease in relative permittivity with increase in measurement frequency. At 100 kHz, the sandwich structured PZT/PMTT/PZT thin film exhibits a relative permittivity of 1510, which is apparently higher than that of the single layer PZT thin film, and lower than that of single layer PMTT thin film. By considering the sandwich structured thin films as consisting of three capacitors in series, i.e.,

$$1/C_s = 1/C_1 + 1/C_2 + 1/C_3 \quad \text{and} \tag{1}$$

$$1/\varepsilon_s = (d_1/\varepsilon_1 + d_2/\varepsilon_2 + d_3/\varepsilon_3)/(d_1 + d_2 + d_3) \tag{2}$$

where C_s, ε_s are the capacitance and relative permittivity of sandwich structured thin film, respectively, C_n, ε_n and d_n ($n = 1, 2, 3$) are the capacitance, relative permittivity and thickness of each constituent layer. In the sandwich structured PZT/PMTT/PZT thin film, the two PZT layers are 100 nm in thickness and the PMTT interlayer is 180 nm. Given the measured relative permittivities of 595 and 2015 at 100 kHz for PZT layer and PMTT interlayer, respectively, the relative permittivity calculated from Eq. (2) is ∼900, which is much lower than the measured relative permittivity (∼1510) for the sandwich structured PZT/PMTT/PZT thin film. This suggests that the sandwich structure can not be simply considered as a series connection of three individual component layers.

4 Conclusions

Sandwich structured PZT/PMTT/PZT thin film has been successfully deposited on Pt/Ti/SiO_2/Si substrate via a combined route involving sol-gel and RF magnetron sputtering. Insertion of the PMTT interlayer suppressed the formation of inhomogeneous "rosette" structure of PZT film on Pt electrode, whereby the inter-diffusion between the top PZT layer and Pt electrode and associated defects are reduced, as confirmed by XPS and SIMS analyses. The sandwich structured PZT/PMTT/PZT thin film shows an apparent decrease in remanent polarization (P_r), a significant reduction in coercive field (E_c) and much improved fatigue resistance, as compared to those of the single layer PZT thin film of the same thickness. It also exhibits a higher relative permittivity than the single layer PZT thin film. However, the sandwich structured thin film cannot be described by a simple capacitor-in-series model of the three individual components layers, suggesting there is a degree of coupling and interaction between the different ferroelectric layers.

Acknowledgment This paper is based upon work supported by the Science and Enggineering Research Council—A* Star, Singapore, under Grant No. 022 107 007. The authors also acknowledge the support of the National University of Singapore.

References

1. J.C. Jiang, X.Q. Pan, W. Tian, C.D. Theis, and D.G. Schlom, *Appl. Phys. Lett.*, **74**, 2851 (1999).
2. D.H. Bao, N. Wakiya, K. Shinozaki, and N. MIzutani, *J. Phys. D-Appl. Phys.*, **35**, L1 (2002).
3. J. Shen and Y.Q. Ma, *J. Appl. Phys.*, **89**, 5031 (2001).
4. T. Hayashi and T. Tanaka, *Japanese J. Appl. Phys.*, **34**, 5100 (1995).
5. E.D. Specht, H.-M. Christen, D.P. Norton, and L.A. Boatner, *Phys. Rev. Lett.*, **80**, 4317 (1998).
6. A. Erbil, Y. Kim, and R.A. Gerhardt, *Phys. Rev. Lett.*, **77**, 1628 (1996).
7. S.-B. Liu, Y.-Q. Li, and M.-D. Liu, *J. Electr. Mater.*, **32**, 1085 (2003).
8. D.-H. Bao, N. Wakiya, K. Shinozaki, and N. Mizutani, *J. Phys. D-Appl. Phys.*, **35**, L1 (2002).
9. T.-L. Ren, L.-T. Zhang, L.-T. Liu, and Z.-J. Li, *J. Sol-Gel. Sci. Technol.*, **24**, 271 (2002).
10. F. Li, J. M. Xue, and J. Wang, *J. Amer. Cerami. Soc.*, **88**, 2769 (2005).
11. H.S. Lee, J.M. Jung, and S.W. Choi, *Ferroelectrics*, **235**, 251 (1999).
12. T. Atsuki, N. Soyama, G. Sasaki, T. Yonezawa, K. Ogi, K. Sameshima, K. Hoshiba, Y. Nakao, and A. Kamisawa, *Japanese J. Appl. Phys.*, **33**, 5196 (1994).
13. H. Doi, T. Atsuki, N. Soyama, G. Sasaki, T. Yonezawa, and K. Ogi, *Japanese J. Appl. Phys.*, **33**, 5159 (1994).
14. M.J. Bozack, *Surf. Sci. Spectra*, **1**, 178 (1992).
15. S.M. Gupta, A.R. Kulkarni, M. Vedpathak, and S.K. Kulkarini, *Mater. Sci. Engg.,* B, **39**, 34 (1996).
16. A. Lezau, B. Skadtchenko, M. Trudeau, and D. Antonelli, *Dalton Trans.*, **21**, 4115 (2003).
17. Z.H. Zhou, J.M. Xue, W.Z. Li, J. Wang, H. Zhu, and J.M. Miao, *J. Appl. Phys.*, **96**, 5706 (2004).
18. I.K. Yoo and S.B. Desu, *Mater. Sci. Engg.* B, **13**, 19 (1992).
19. W.L. Warren, D. Dimos, B.A. Tuttle, R.D. Nasby, and G.E. Pike, *Appl. Phys. Lett.*, **65**, 1018 (1994).